2.F *Nuclear Physics* **A165** (1971) 240—258; © *North-Holland Publishing Co., Amsterdam*

(d, ^{6}Li) REACTIONS ON p AND sd SHELL NUCLEI AND THEIR INTERPRETATION BY FINITE-RANGE DWBA

H. H. GUTBROD, H. YOSHIDA † and R. BOCK
Max-Planck-Institut für Kernphysik, Heidelberg
and
Physikalisches Institut der Universität Marburg

Received 28 December 1970

Abstract: The (d, ^{6}Li) reaction on ^{10}B, ^{11}B, ^{12}C, ^{16}O, ^{19}F, ^{28}Si and ^{40}Ca has been investigated with the 19.5 MeV deuteron beam of the MPI Emperor tandem Van de Graaff. The measured angular distributions are analyzed by finite-range DWBA calculations. Spectroscopic factors for the α-cluster transfer have been calculated from shell-model wave functions for the target nuclei. The theoretical cross sections are found to be very sensitive to the choice of the model for ^{6}Li. The cluster model leads to cross sections which are strongly enhanced compared to the shell-model predictions. They reproduce the absolute experimental cross sections of the ground state transitions for the target nuclei from ^{12}C to ^{40}Ca. However, the experimental (d, ^{6}Li) cross section on the ^{10}B target is much larger than predicted and the angular distribution cannot be described. This indicates a more complicated reaction mechanism in this case.

E NUCLEAR REACTIONS ^{10,11}B, ^{12}C, ^{16}O, ^{19}F, ^{28}Si, ^{40}Ca(d, ^{6}Li), $E = 19.5$ MeV; measured $\sigma(E_{^6\mathrm{Li}}, \theta)$. Enriched and natural targets.

1. Introduction

The (d, ^{6}Li) reaction has the following properties which make it suitable for the investigation of the α-cluster structure of nuclei:

(i) The reaction proceeds predominantly via a direct mechanism. This can be concluded from the angular distribution measured by Denes *et al.* [3]) at about 15 MeV and Gerhard *et al.* [4]) at 21 MeV incident energy.

(ii) It can be assumed that there is a large probability for finding a deuteron and an α-cluster in ^{6}Li. The momentum distribution obtained from electron scattering shows a strong isolation of these clusters [2]). Therefore, the four nucleons transferred in the (d, ^{6}Li) reaction can be considered as an α-cluster in its lowest state, and the cross section for the pick-up process should be determined by the reduced α-particle width of the target nucleus.

(iii) Because of the strong absorption of ^{6}Li in nuclei the (d, ^{6}Li) reaction is localized mainly at the surface of the nucleus.

The (d, ^{6}Li) experiments to be reported here were performed at 19.5 MeV. Some

† On leave from Osaka University, Osaka, Japan.

target nuclei between ^{10}B and ^{40}Ca representing the range from the p to the sd shell have been selected. The data were analyzed by means of a finite-range DWBA code [5]) assuming a simple α-transfer process. Shell-model wave functions including configuration mixing were used for describing the target and final nuclei. Since the finite-range theory is able to predict absolute cross sections, the α-cluster structure of all target nuclei can be investigated consistently.

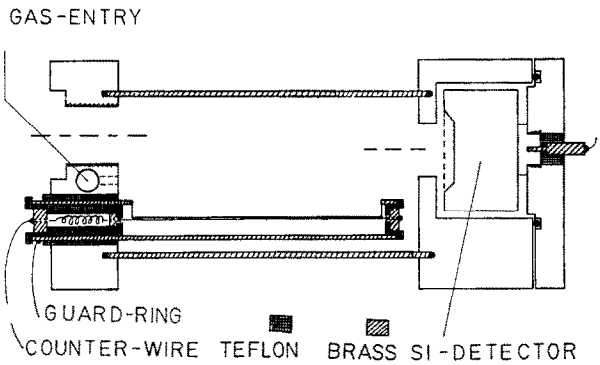

Fig. 1. Design of the proportional counter telescope.

2. Experimental procedure and results

Angular distributions and absolute cross sections were measured for the (d, ^{6}Li) reactions on ^{10}B, ^{11}B, ^{12}C, ^{16}O, ^{19}F, ^{28}Si and ^{40}Ca at an incident energy of 19.5 MeV. The deuterons were accelerated by the Heidelberg MP tandem Van de Graaff and entered a 50 cm scattering chamber through a collimating system, which produced a beam spot of 1×2 mm^2 on the target. For the measurements on ^{10}B and ^{11}B, carbon-free self-supporting foils of about 60–80 μg/cm^2 were used. In the case of (d, ^{6}Li) on ^{16}O the target was a 150 μg/cm^2 SiO_2 foil and for ^{19}F and ^{40}Ca CaF_2 was evaporated on a backing of Al.

The lithium isotopes were detected and identified by a $\Delta E-E$ telescope with a proportional counter as a ΔE counter and a solid-state detector as an E-detector (fig. 1). The pulses were processed by two-dimensional analysis in a 16 K multichannel analyzer. The resolution of the ΔE counter was about 4 %, and because of the very thin entrance window it was possible to separate completely ^{6}Li and ^{7}Li down to an energy of 2–3 MeV. The energy resolution of $\approx$ 120 keV (FWHM) was mainly determined by kinematics and target thickness. The acceptance angle in the reaction plane was 0.2°. The measured angular distributions have an absolute angular uncertainty of less than $\pm 1.0°$ c.m.

Absolute cross sections were determined to better than 20 % by measuring Rutherford scattering of 12 MeV ^{16}O ions on the targets used. By this method uncertainties in the determination of the target thickness and the solid angle cancel.

Some (d, ^{6}Li) spectra are shown in fig. 2. The measured angular distributions are contained in fig. 3. The ground state transitions on ^{12}C, ^{19}F and ^{40}Ca show regular oscillations. This supports the assumption of a direct mechanism for the reaction.

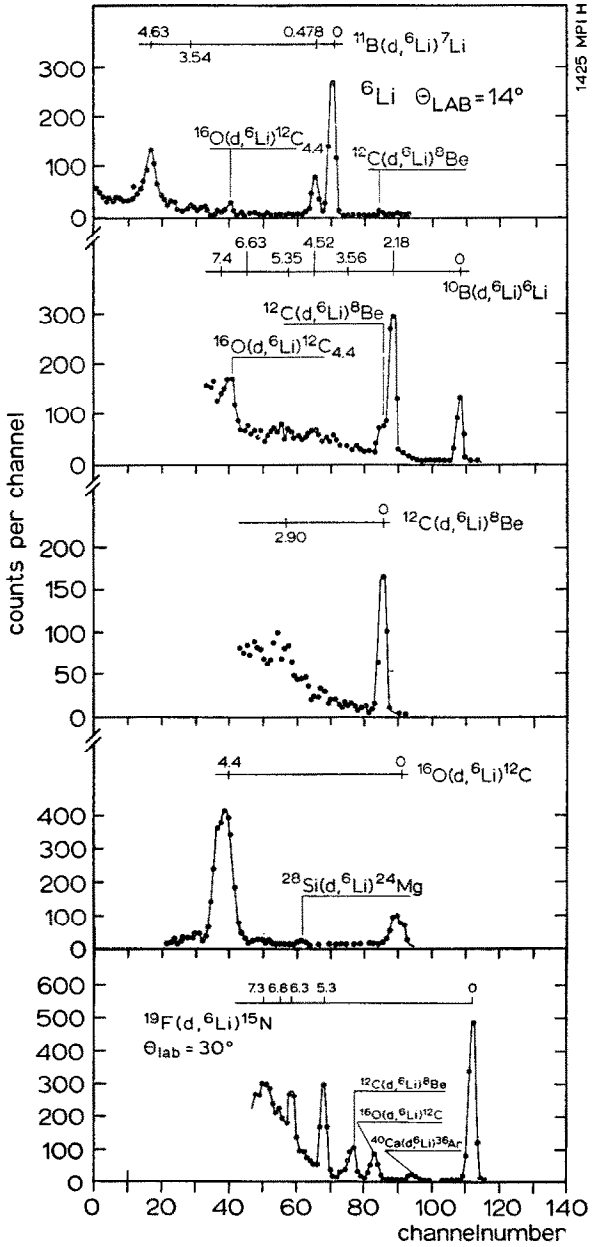

Fig. 2. Energy spectra of ^{6}Li produced by (d, ^{6}Li) reactions on different target nuclei.

The ^{10}B(d, ^{6}Li)^{6}Li *reaction.* For the ground state transition the particles in the exit channel are identical. Therefore, the ground state transition is expected to be enhanced compared with other transitions. The higher $T = 0$ states in ^{6}Li are pop-

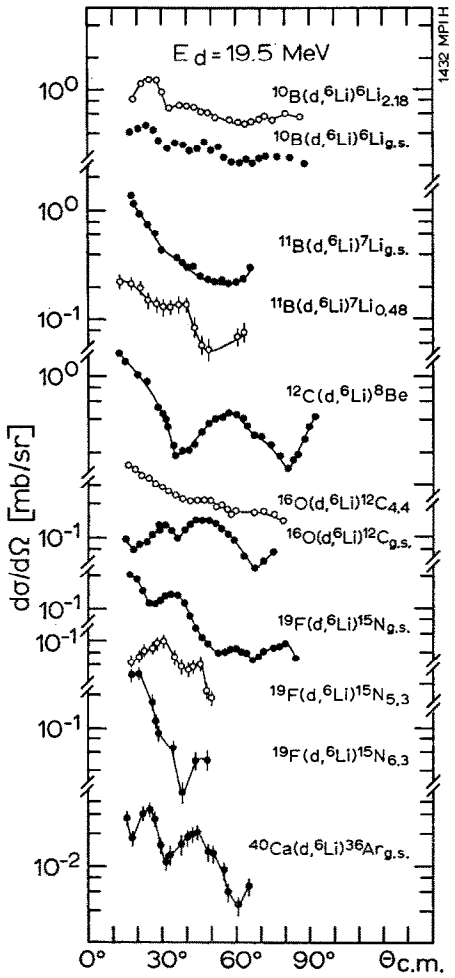

Fig. 3. Angular distributions of (d, ^{6}Li) reactions from different target nuclei.

ulated weakly. Their spectra have a large width because of the short lifetime of these states. There is no indication for the population of the $T = 1$ state at 3.56 MeV in agreement with the $\Delta T = 0$ selection rule. The continuum in the ^{6}Li spectrum starting at about 2 MeV is presumably due to the break-up of ^{10}B into ^{6}Li and α-particle (fig. 2). The angular distribution (fig. 3) is very flat for the transitions to both the 1^+ and the 3^+ state. In the 3^+ to 1^+ transition the values $l_{tr} = 2$ and 4 for the transferred angular momentum are possible, in the 3^+ to 3^+ transition there are

$l_{tr} = 0, 2, 4$ and they contribute incoherently. The angular distribution is expected to be symmetric to 90° for the ground state transition because of the identity of the particles in the exit channel.

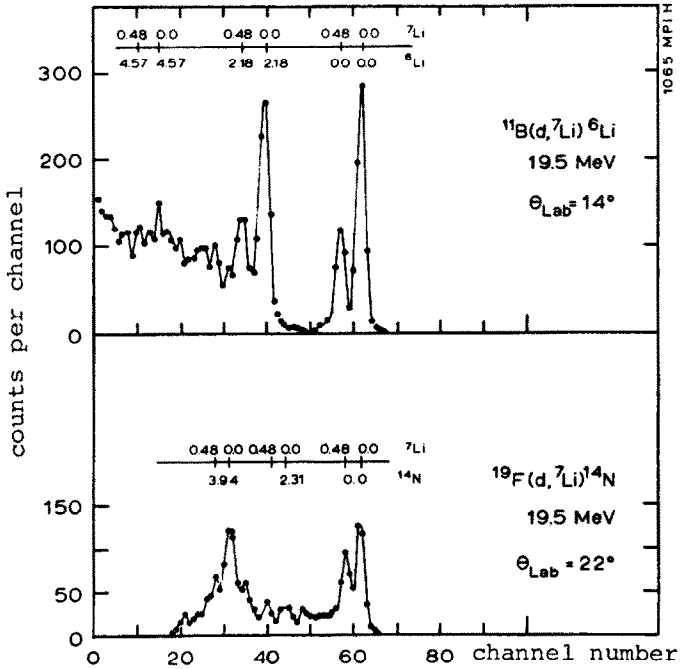

Fig. 4. Energy spectra of ^{7}Li produced by (d, ^{7}Li) on ^{11}B and ^{19}F.

The ^{11}B(d, ^{6}Li)^{7}Li *reaction.* The relative population of the states in ^{7}Li (see fig. 2) is in agreement with shell-model predictions [6]). For the ground state transitions angular momentum values of $l_{tr} = 0$ and 2 are possible. The ratio of the excitations of the $\frac{3}{2}^-$ state to the $\frac{1}{2}^-$ state in ^{7}Li is found to be 2 : 1, in agreement with the $2J+1$ rule. The ^{6}Li spectrum does not contain any break-up contributions whereas in the ^{7}Li spectrum (see fig. 4) the break-up of ^{11}B into ^{7}Li and α-particle may explain the continuum above 2 MeV excitation energy.

The forward rise in the angular distributions of ^{11}B(d, ^{6}Li)^{7}Li and ^{11}B(d, ^{7}Li)^{6}Li (fig. 5) may have two different explanations. (i) Because the ^{7}Li detected at forward angles corresponds to backward angles of ^{6}Li, the ^{11}B(d, ^{6}Li)^{7}Li angular distribution may have a backward rise and hence a strong part symmetric to 90°, i.e. the reaction would be expected to proceed to a large extent by a compound nucleus mechanism. (ii) The forward rise in the angular distributions is due to a direct mechanism for both the (d, ^{6}Li) and the (d, ^{7}Li) reaction. The spectra show that the population of the levels is not proportional to $2J+1$, especially not in (d, ^{7}Li) where the 3^+ state in ^{6}Li should be excited much stronger than the 1^+. Further-

more, from ^{7}Li induced reactions in ^{12}C [ref. ^{7})] it is known that a five-nucleon transfer can occur with a large cross section. Therefore we assume that the reaction ^{11}B(d, ^{6}Li)^{7}Li, too, proceeds mainly by a direct mechanism.

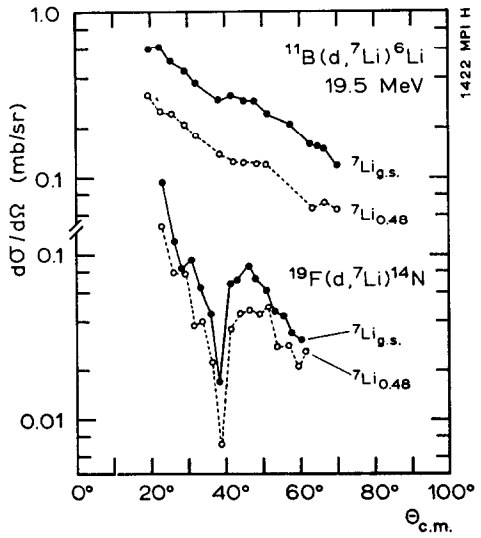

Fig. 5. Angular distribution of the ^{11}B(d, ^{7}Li)^{6}Li and the ^{19}F(d, ^{7}Li)^{14}N reactions.

The ^{12}C(d, ^{6}Li)^{8}Be *reaction.* At forward angles the most prominent peak in the spectrum (fig. 2) belongs to the $l_{tr} = 0$ ground state transition. At higher angles, the $l_{tr} = 2$ transition to the broad 2^+ state at 2.9 MeV in ^{8}Be becomes dominant. The angular distribution of the ground state transition does not change noticeably compared to the 21 MeV data [4]).

The ^{16}O(d, ^{6}Li)^{12}C *reaction.* The population of the 2^+ state in ^{12}C is about five times stronger than the ground state transition and agrees with the prediction based on shell-model calculations [6]). Some spectra have been measured at a deuteron energy of 20 MeV. At this energy a weak population of the 0^+ state at 7.65 MeV can be observed. Since this state is assumed to have mainly a $(sd)^4(p)^{-8}$ configuration, the ratio $\sigma/\sigma_{g.s.}$ should give information on the 4p-4h admixture to the ground state wave function of ^{16}O. The ratio is observed to be 0.12 at 35°. This should not be taken too seriously because one expects a contribution from a compound reaction of about 20 % from an analysis of the inverse reaction ^{12}C(^{6}Li, d)^{16}O [ref. ^{8})].

The ^{19}F(d, ^{6}Li)^{15}N *reaction.* Beside the $\frac{1}{2}^-$ ground state of ^{15}N, the two unresolved states at 5.3 MeV ($\frac{1}{2}^+$, $\frac{5}{2}^+$) and the $\frac{3}{2}^-$ state at 6.3 MeV are populated. The diffraction structures in the angular distributions (fig. 3) indicate under small angles the difference of the transferred angular momenta. On that target nucleus the (d, ^{7}Li) reaction is not hindered by a too negative Q-value. This reaction is even comparable

in cross section with the (d, ^{6}Li) reaction. The ^{19}F(d, ^{7}Li)^{14}N ground state transition (fig. 5) has a similar shape of the angular distribution as the ^{19}F(d, ^{6}Li)^{15}N$_{6.3}$ transition. We conclude that in ^{19}F the α-cluster configuration is not pronounced.

The ^{28}Si(d, ^{6}Li)^{24}Mg *and* ^{40}Ca(d, ^{6}Li)^{36}Ar *reactions.* By means of a SiO_2 and a CaF_2 target we could observe these reactions together with ^{16}O(d, ^{6}Li)^{12}C and ^{19}F(d, ^{6}Li)^{15}N. In ^{28}Si(d, ^{6}Li)^{24}Mg the cross section drops from 20 μb/sr at 14° to 1 μb/sr at 21° c.m., indicating a strong diffraction structure in the angular distribution. The angular distribution of ^{40}Ca(d, ^{6}Li)^{36}Ar shows a strong decrease at larger angles indicating the pronounced surface localization of this reaction.

3. DWBA analysis

3.1. THEORY

Denoting the pick-up reaction as B(b, a)A, the DWBA cross section can be written as follows [10]):

$$\frac{\mathrm{d}\sigma(\mathrm{b}\to\mathrm{a})}{\mathrm{d}\Omega} = \left\{\frac{2s_\mathrm{a}+1}{2s_\mathrm{b}+1}\right\} \sum_l S_l \sigma_l(\theta), \tag{1}$$

where s_a and s_b are the spins for particle a and b, respectively. The quantity $\sigma_l(\theta)$ is defined by [11])

$$\sigma_l(\theta) = \frac{\mu_\mathrm{a}\mu_\mathrm{b}}{(2\pi\hbar^2)^2}\,\frac{k_\mathrm{a}}{k_\mathrm{b}} \sum_m |\beta_{lm}(\theta)|^2. \tag{2a}$$

Here μ_a and μ_b are the reduced mass of particle a and b, and the quantity $\beta_{lm}(\theta)$ is defined as in ref. [11]):

$$i^l(2l+1)^{\frac{1}{2}}\beta_{lm}(\theta) = J\int \mathrm{d}\boldsymbol{r}_\mathrm{aA}\int \mathrm{d}\boldsymbol{r}_\mathrm{bB}\,\chi_\mathrm{b}^{(-)*}(\boldsymbol{k}_\mathrm{b}, \boldsymbol{r}_\mathrm{bB}) f_{lm}(\boldsymbol{r}_\mathrm{bB}, \boldsymbol{r}_\mathrm{aA})\chi_\mathrm{a}^{(+)}(\boldsymbol{k}_\mathrm{a}\boldsymbol{r}_\mathrm{a}). \tag{2b}$$

When the colliding particles in the ingoing or outgoing channel are identical as in the case of the reaction ^{10}B(d, ^{6}Li)^{6}Li, $\sigma_l(\theta)$ is replaced by

$$\sigma_l(\theta) = \frac{\mu_\mathrm{a}\mu_\mathrm{b}}{(2\pi\hbar^2)^2}\,\frac{k_\mathrm{a}}{k_\mathrm{b}} \sum_m |\beta_{lm}(\theta)|^2 + |\beta_{lm}(\pi-\theta)|^2 + B_l\,\mathrm{Re}\,\{\beta_{lm}(\theta)\beta_{lm}^*(\pi-\theta)\}, \tag{2c}$$

where B_l is given by

$$B_l = 2(2J_1+1)\begin{pmatrix} l & 0 & J_1 \\ 0 & S_\mathrm{b} & J_\mathrm{A} \\ J_1 & J_\mathrm{A} & J_\mathrm{B} \end{pmatrix}.$$

The form factor f_{lm} and the spectroscopic factor S_l are given as the expansion of the effective interaction into terms corresponding to the transfer to a target nucleus of total

angular momentum j comprising an orbital part l and a spin part s:

$$J\langle I_B M_B, s_b m_b|V|I_A M_A, s_a m_a\rangle$$
$$= \sum_{lsj} \langle I_A\, jM_A M_B - M_A|I_B M_B\rangle\langle lsmm_a - m_b|jM_B - M_A\rangle$$
$$\times \langle s_a s_b\, m_a - m_b|sm_a - m_b\rangle(-)^{s_b - m_b} i^{-l} A_{lsj} f_{lm}(\boldsymbol{r}_{bB}, \boldsymbol{r}_{aA}). \tag{3}$$

The spectroscopic factor S_l defined in eq. (1) is connected with the spectroscopic amplitude A_{lsj} of eq. (3) by

$$S_l = \frac{1}{2s_a+1}\binom{n}{4}\sum_{sj}|A_{lsj}|^2, \tag{4}$$

for the four-nucleon transfer reaction. Here n denotes the number of active nucleons in the nucleus B.

In order to obtain the explicit form for the form factor f_{lm} and spectroscopic amplitude A_{lsj}, initial and final state wave functions must be written down explicitly. For the present calculation, the particle a is the ^{6}Li particle and b is the deuteron and we have used shell-model wave functions of the LS coupling scheme for the initial and final nucleus. For the ^{6}Li ground state, the simple configuration [13]) has been assumed:

$$|s_a m_a\rangle_{\text{shell}} = |(s^4)p^2[2]^1{}^3S_1\rangle. \tag{5}$$

So the ^{6}Li state is considered to be composed of an α-particle (four particles in the s-shell) and two particles in the p-shell coupled to total angular momentum $S_a = 1$. The residual and the target nucleus states can be generally written as

$$|I_A M_A\rangle_{\text{shell}} = \sum_{[\lambda_A]} C_A|l_f^{n-4}[\lambda_A]T_A S_A L_A; I_A M_A\rangle,$$
$$|I_B M_B\rangle_{\text{shell}} = \sum_{[\lambda_B]} C_B|l_f^n[\lambda_B]T_B S_B L_B; I_B M_B\rangle$$
$$= \sum_{[\lambda_B][\lambda'_A][\lambda_1]} C_B\langle l_f^n[\lambda_B]T_B S_B L_B\{|l_f^{n-4}[\lambda'_A]T'_A S'_A L'_A, l_f^4[\lambda_1]T_1 S_1 L_1\rangle \tag{6a}$$
$$\times \langle(S'_A L'_A)I'_A, (S_1 L_1)I_1; I_B|(S'_A S_1)S_B, (L'_A L_1)L_B; I_B\rangle$$
$$\times |l_f^{n-4}[\lambda'_A]T'_A(S'_A L'_A)I'_A, l_f^4[\lambda_1]T_1(S_1 L_1)I_1; I_B M_B\rangle.$$

Here C_A and C_B are the mixing amplitudes of the state and the quantity

$$\langle l_f^n[\lambda_B]T_B S_B L_B\{|l_f^{n-4}[\lambda_A]T_A S_A L_A, l_f^4[\lambda_1]T_1 S_1 L_1\rangle$$

is the fractional parentage coefficient to pick up four nucleons and

$$\langle(S_A L_A)I_A, (S_1 L_1)I_1; I_B|(S_A S_1)S_B, (L_A L_1)L_B; I_B\rangle$$

is related to the 9*j* symbol by the relation:

$$\langle (S_A L_A) I_A, (S_1 L_1) I_1; I_B | (S_A S_1) S_B, (L_A L_1) L_B; I_B \rangle = \sqrt{(2I_A+1)(2I_1+1)(2S_B+1)(2L_B+1)} \begin{Bmatrix} S_A & L_A & I_A \\ S_1 & L_1 & I_1 \\ S_B & L_B & I_B \end{Bmatrix}. \quad (7)$$

The summation $[\lambda]$ in eq. (6) includes also the spin S and orbital angular momentum L. To calculate the spectroscopic amplitude A_{lsj} and form factor f_{lm}, the eqs. (5), (6a) and (6b) are inserted into the left-hand side of eq. (3) and the integrations are performed with respect to the coordinates of the nuclei A and b. The resulting four-nucleon wave functions are expanded into the c.m. and the relative motion by making use of the Talmi coefficient. The integration over the relative coordinate can also be performed when assuming the direct interaction to be dependent only on the coordinate $r_{\alpha b}$ connecting the c.m. of four nucleons and the outgoing particle. Then we get finally [6])

$$\begin{aligned} A_{lsj} = {} & \frac{3}{2\sqrt{2}} \sqrt{(2s_a+1)} \sum_{\substack{[\lambda_A][\lambda_B] \\ [\lambda_{12}][\lambda_{34}]}} C_A C_B \left(\frac{B}{A}\right)^{\frac{1}{2}(N_{12}+L_1)} \langle l_f^n [\lambda_B] T_B S_B L_B \{ | l_f^{n-4} [\lambda_A] T_A S_A L_A \\ & \times l_f^4 [4] 00 L_1 \rangle \langle (S_A L_A) I_A, (0 L_1) L_1; I_B | (S_A 0) S_B, (L_A L_1) L_B; I_B \rangle \delta_{S0} \delta_{jL_1} \delta_{lL_1} \\ & \times \langle l_f^4 [4] 00 L_1 \{ | l_f^2 [\lambda_{12}] T_{12} S_{12} L_{12}, l_f^2 [\lambda_{34}] T_{34} S_{34} L_{34} \rangle \\ & \times \langle S^4 [4]^{11} S \{ | S^2 [2] T_{12} S_{12} 0, S^2 [2] T_{34} S_{34} 0 \rangle \langle N_1 L_{12} N_2 L_{34}; L_1 | N_{12} L_1 00; L_1 \rangle \\ & \times \langle n_f l_f n_f l_f; L_{12} | N_1 L_{12} 00; L_{12} \rangle \langle n_f l_f n_f l_f; L_{34} | N_2 L_{34} 00; L_{34} \rangle; \end{aligned} \quad (8a)$$

$$f_{lm}(r_{bB}, r_{aA}) = \Phi^*_{N_{12}l}(r_{\alpha A}) V(|r_{\alpha b}|) \Phi_{10}(r_{\alpha b}), \quad (8b)$$

where

$$\langle n_f l_f n_f l_f; L_{12} | N_1 L_{12} 00; L_{12} \rangle$$

is the Talmi coefficient [14]). From the parentage coefficient and the 9*j* symbol in eqs. (8), we get easily the relation

$$T_A = T_B, \quad S_A = S_B, \quad T_{12} = T_{34}, \quad S_{12} = S_{34}.$$

From the energy conservation in the Talmi coefficient, the relation

$$2N_{12} + L_1 = 4(2n_f + l_f)$$

is derived. The bound state wave function Φ_{Nl} which describes the c.m. motion of the four nucleons, is specified by the number of radial nodes N and orbital angular momentum l. In deriving eq. (8a), the c.m. coordinate R of each nucleus is separated out from the shell-model wave function by the relation [15])

$$\psi_L^{\text{shell}} = \Phi_{00}(R) \psi_L, \quad (9)$$

from which the factors $(B/A)^{\frac{1}{2}(N_{12}+L_1)}$ and $\frac{3}{2}$ arise in eq. (8a). The coordinates

$r_{\alpha A}$ and $r_{\alpha b}$ in eq. (8) are connected with the relative coordinates r_{bB} and r_{aA} by the relations

$$r_{\alpha A} = \frac{1}{4}\frac{B}{A+a}(ar_{aA} - br_{bB}),$$

$$r_{\alpha b} = \frac{1}{4}\frac{a}{A+a}(Ar_{aA} - Br_{bB}), \tag{10}$$

where a, A, ... represent the masses of the corresponding particles.

3.2. CALCULATION OF THE FORM FACTOR

In the numerical calculations, the bound state wave function $\Phi_{N_{12}l}$ in eq. (8b) is replaced by the wave functions solved in a Woods-Saxon potential with parameters $r_0 = 1.25$ fm and $a = 0.65$ fm so as to fit the empirical α-particle separation energy by adjusting the potential depth.

Electron scattering data support an isolation of the clusters in ^{6}Li as it is described in the cluster model for ^{6}Li [ref. ^{16})]. In our calculation there is only the form factor which depends on the relative coordinates of the α-particle and the deuteron in ^{6}Li. Therefore the shell-model wave function Φ_{10} in eq. (8b) has to be replaced by the cluster wave function Φ_{00}:

$$\Phi_{00}(r) = r^2[\exp(-c_1 r^2) + c_2 \exp(-c_3 r^2)]. \tag{11}$$

The notation Φ_{00} instead of Φ_{10} is used here corresponding to the radial number of node $N = 0$. The parameters c_1, c_2 and c_3 were determined by the variational method in ref. ^{16}).

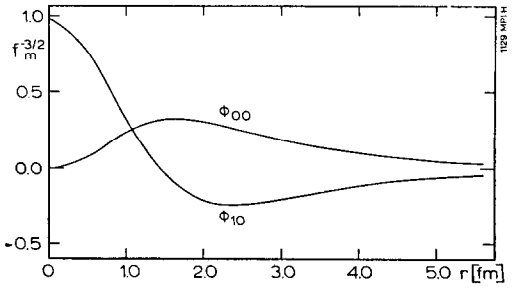

Fig. 6. Wave functions Φ_{00} and Φ_{10} describing the relative motion of α and d. The Φ_{00} is deduced from the cluster model, Φ_{10} from the shell model.

In this paper the wave function Φ_{00} has been simulated by the wave function calculated in a Woods-Saxon potential assuming that the particle motion is described by the radial node $N = 0$ and the angular momentum $L = 2$. The result is shown

in fig. 6 together with the shell-model prediction. The parameters of the direct interaction $V(r)$ with the form

$$V(r) = V_D \frac{1}{1+\exp[(r-r_D)/a]} \tag{12}$$

are determined as $V_D = 99.46$ MeV with the fixed parameter $a = 0.65$ fm and $R_D = 1.58$ fm.

3.3. CALCULATIONS OF THE SPECTROSCOPIC FACTORS

For the calculation of S_l given by eqs. (4) and (8), the results of shell-model calculations are used to describe the targets and residual nuclear states. They are shown in table 1. All states are described by LS coupling representation except for the last

TABLE 1

Wave functions for the calculation of S_l

$\|^6\mathrm{Li}\rangle_{3+}$	$= \mathrm{p}^2[2]^{13}\mathrm{D}_3$
$\|^7\mathrm{Li}\rangle_{\frac{3}{2}-}$	$= \mathrm{p}^3[3]^{22}\mathrm{P}_{\frac{3}{2}}$
$\|^8\mathrm{Be}\rangle_{0+}$	$= \mathrm{p}^4[4]^{11}\mathrm{S}_0$
$\|^{10}\mathrm{B}\rangle_{3+}$	$= -0.421\ \mathrm{p}^6[42]^{13}\mathrm{D}_{13} + 0.678\ \mathrm{p}^6[42]^{13}\mathrm{D}_{113} - 0.481\ \mathrm{p}^6[42]^{13}\mathrm{F}_3$ $-0.204\ \mathrm{p}^6[42]^{13}\mathrm{G}_3$ [ref. [17])]
$\|^{11}\mathrm{B}\rangle_{\frac{3}{2}-}$	$= -0.672\ \mathrm{p}^7[43]^{22}\mathrm{P}_{\frac{3}{2}} + 0.741\ \mathrm{p}^7[43]^{22}\mathrm{D}_{\frac{3}{2}}$ [ref. [18])]
$\|^{12}\mathrm{C}\rangle_{0+}$	$= \mathrm{p}^8[44]^{11}\mathrm{S}_0$
$\|^{12}\mathrm{C}\rangle_{2+}$	$= \mathrm{p}^8[44]^{11}\mathrm{D}_2$
$^{15}\mathrm{N}\rangle_{\frac{1}{2}-}$	$= \mathrm{p}^{11}[443]^{22}\mathrm{P}_{\frac{1}{2}}$
$^{16}\mathrm{O}\rangle_{0+}$	$= \mathrm{p}^{12}[444]^{11}\mathrm{S}_0$
$\|^{19}\mathrm{F}\rangle_{\frac{1}{2}+}$	$= (\mathrm{p}^{12})(-0.4343\ \mathrm{s}^3[3]^{22}\mathrm{S}_{\frac{1}{2}} - 0.7777\ \mathrm{d}^2\mathrm{s}[3]^{22}\mathrm{S}_{\frac{1}{2}} - 0.3438\ \mathrm{d}^3[3]^{22}\mathrm{S}_{\frac{1}{2}})$ [ref. [19])]
$\|^{36}\mathrm{Ar}\rangle_{0+}$	$= -\sqrt{0.856}(\mathrm{s}^4_{00}\mathrm{d}^4_{00})_{00} - \sqrt{0.12}(\mathrm{s}^2_{01}\mathrm{d}^6_{01})_{00} - \sqrt{0.01}(\mathrm{s}^2_{10}\mathrm{d}^6_{10})_{00}$ $+\sqrt{0.008}(\mathrm{s}^3_{\frac{1}{2}\frac{1}{2}}\mathrm{d}^5_{\frac{1}{2}\frac{1}{2}})_{00} - \sqrt{0.006}\,\mathrm{d}^8_{00}$ [ref. [20])]
$\|^{40}\mathrm{Ca}\rangle_{0+}$	$= (\mathrm{s}^4_{00}\mathrm{d}^8_{00})_{00}$

two cases, where the ground states $|^{36}\mathrm{Ar}\rangle$ and $|^{40}\mathrm{Ca}\rangle$ are described by the *jj* coupling representation of the sd shell $(\mathrm{s}^n_{j_1t_1}\mathrm{d}^m_{j_2t_2})_{JT}$ with the assumption of an inert ^{28}Si core. The calculation of the spectroscopic factor S_l is made straightforward for p-shell nuclei by using eqs. (4) and (8a). In the calculation of the α-particle reduced width the table of parentage coefficients by Elliot *et al.* [21]) and also the results by Rotter [6]) and by Honda *et al.* [22]) are used. We have assumed the simplest configuration for the ^{12}C and ^{16}O ground state. A more detailed calculation for ^{12}C states which takes into

account lower symmetry terms gives the following form [17]) for the ^{12}C ground state:

$$|^{12}\mathrm{C}\rangle_{0^+} = 0.896\mathrm{p}^8[44]^1\mathrm{S}_0 + 0.413\mathrm{p}^8[431]\mathrm{P}_0 - 0.146\mathrm{p}^8[422]^1\mathrm{D}_0 + 0.039\mathrm{p}^8[422]^1\mathrm{S}_0 + 0.060\mathrm{p}^8[332]^1\mathrm{P}_0 .$$

Using this wave function for the ^{12}C ground state the calculated S_l is reduced by 20 % for the reaction ^{16}O(d, ^{6}Li)^{12}C.

For ^{16}O Ellis *et al.* [23]) have calculated the low-lying levels taking into account 2p-2h components. The result for the ^{16}O ground state is:

$$|^{16}\mathrm{O}\rangle_{0^+} = 0.884\mathrm{p}^{12} + 0.294\mathrm{p}^{10}(^1\mathrm{S})\mathrm{d}^2(^1\mathrm{S}) - 0.232\mathrm{p}^{10}(^3\mathrm{P})\mathrm{d}^2(^3\mathrm{P}) + 0.191\mathrm{p}^{10}(^1\mathrm{S})\mathrm{d}^2(^1\mathrm{S}) + 0.112\mathrm{p}^{10}(^1\mathrm{D})\mathrm{d}^2(^1\mathrm{D}) + 0.076\mathrm{p}^{10}(^1\mathrm{S})\mathrm{S}^2(^1\mathrm{S}).$$

The use of this wave function for the ^{16}O ground state causes the change of the form factor $\Phi_{N_{12}}$ in eq. (8b) for the reaction ^{16}O(d, ^{6}Li)^{12}C:

$$\Phi_{20} \to 0.884\,\Phi_{20} - 0.069\,\Phi_{30} \text{ ground state of } ^{12}\mathrm{C},$$

$$\Phi_{12} \to 0.884\,\Phi_{12} - 0.061\,\Phi_{22} \text{ first excited state.}$$

It is found in the numerical calculations that the second terms which come from 2p-2h components give a negligible contribution to the cross section. The ratio of the calculated cross sections without and with the second term in the form factor is 0.80 at $\theta_{\mathrm{c.m.}} = 30°$ for the transition leading to the ^{12}C ground state and is 0.81 for the transition to ^{12}C first excited state at the same angle. So in the present analysis only the simplest configurations are taken for both ^{12}C and ^{16}O states.

For sd shell nuclei eq. (8a) must be extended for the calculation of S_l. For the case of the reaction ^{19}F(d, ^{6}Li)^{15}N the coefficient

$$\langle l_f^n[\lambda_\mathrm{B}]T_\mathrm{B}\,S_\mathrm{B}\,L_\mathrm{B}\{|l_f^{n-4}[\lambda_\mathrm{A}]T_\mathrm{A}\,S_\mathrm{A}\,L_\mathrm{A}\,,\, l_f^4[4]00L_1\rangle$$

in eq. (8a) must be replaced by

$$\frac{1}{4}\binom{12}{1}^{\frac{1}{2}}\binom{15}{4}^{-\frac{1}{2}}\langle \mathrm{p}^{12}[444]^1\mathrm{S}\{|\mathrm{P}^{11}[443]^2\mathrm{P},\,\mathrm{P}\rangle$$

and also the coefficient

$$\langle l_f^4[4]00L_1\{|l_f^2[\lambda_{12}]T_{12}\,S_{12}\,L_{12}\,,\, l_f^2[\lambda_{34}]T_{34}\,S_{34}\,L_{34}\rangle$$

must be replaced by

$$(-)^{T_{12}+S_{12}}\sqrt{\frac{2}{3}\,\frac{2L_{34}+1}{2L_{12}+1}}\,\langle(\mathrm{sd})^3[3]^2\mathrm{S}\{|(\mathrm{sd})^2[2]T_{12}\,S_{12}\,L_{12}\,,\,(\mathrm{sd})\rangle$$

and finally the Talmi coefficients by corresponding s, d or p shell coefficients. The relation $2N_{12}+L_1 = 7$ holds in this case.

For the case of the reaction ^{40}Ca(d, ^{6}Li)^{36}Ar, the spectroscopic amplitude A_{lsj} can be calculated by the use of the transformation coefficients from the *jj* to the *LS* coupling scheme. The result is

$$A_{000} = \tfrac{3}{2}\sqrt{\tfrac{1}{2}(2s_a+1)}\left(\frac{B}{A}\right)^4\binom{12}{4}^{-\frac{1}{2}}\sum_{k=1}^{5}B^{(k)},$$

where

$$\begin{aligned}
B^{(1)} = {} & -\sqrt{0.856}\binom{8}{4}^{\frac{1}{2}}\langle \mathrm{d}^8(00)\{|\mathrm{d}^4(00), \mathrm{d}^4(00)\rangle \\
& \times \sum_{I_{12}T_{12}S_{12}} \langle \mathrm{d}^4(00)\{|\mathrm{d}^2(I_{12}\,T_{12}), \mathrm{d}^2(I_{12}\,T_{12})\rangle \\
& \times \langle (\tfrac{1}{2}2)\tfrac{3}{2}, (\tfrac{1}{2}2)\tfrac{3}{2}; I_{12}|(\tfrac{1}{2}\tfrac{1}{2})S_{12}, (22)L_{12}, I_{12}\rangle^2 \\
& \qquad \times \langle \mathrm{s}^4[4]^{11}\mathrm{S}\{|\mathrm{s}^2[2]T_{12}\,S_{12}\,0, \mathrm{s}^2[2]T_{12}\,S_{12}\,0\rangle \\
& \times \langle 0202; L_{12}|N_1\,L_{12}\,00; L_{12}\rangle^2\langle N_1\,L_{12}\,N_1\,L_{12}; 0|4000; 0\rangle \\
& \qquad \times \langle (S_{12}\,L_{12})I_{12}, (S_{12}\,L_{12})I_{12}; 0|(S_{12}\,S_{12})0, (L_{12}\,L_{12})0; 0\rangle,
\end{aligned}$$

$$\begin{aligned}
B^{(2)} = {} & -\sqrt{0.12}\binom{8}{2}^{\frac{1}{2}}\binom{4}{2}\langle \mathrm{s}^4(00)\{|\mathrm{s}^2(01), \mathrm{s}^2(01)\rangle\langle \mathrm{d}^8(00)\{|\mathrm{d}^6(01), \mathrm{d}^2(01)\rangle \\
& \times \langle (11)0, (11)0; 0|(11)0, (11)0; 0\rangle\langle (\tfrac{1}{2}0)\tfrac{1}{2}, (\tfrac{1}{2}0)\tfrac{1}{2}; 0|(\tfrac{1}{2}\tfrac{1}{2})0, (00)0; 0\rangle \\
& \times \langle (\tfrac{1}{2}2)\tfrac{3}{2}, (\tfrac{1}{2}2)\tfrac{3}{2}; 0|(\tfrac{1}{2}\tfrac{1}{2})0, (22)0; 0\rangle\langle \mathrm{s}^4[4]^{11}\mathrm{S}\{|\mathrm{s}^2[2]^{31}\mathrm{S}, \mathrm{s}^2[2]^{31}\mathrm{S}\rangle \\
& \times \langle 1010; 0|2000; 0\rangle\langle 0202; 0|2000; 0\rangle\langle 2020; 0|4000; 0\rangle
\end{aligned}$$

with similar expressions for other coefficients $B^{(3)}$, $B^{(4)}$ and $B^{(5)}$. It is found in the numerical calculation for $B^{(k)}$ that all the $B^{(k)}$ ($k = 1 \ldots 5$) have the same sign showing that the configuration mixing favours the alpha-clustering in the nucleus.

4. Choice of the optical potential

For the deuteron optical potential parameters, the results of deuteron scattering analyses on target nuclei ^{12}C, ^{16}O, ^{19}F [ref. [3])], ^{10}B, ^{11}B [ref. [24])] and ^{40}Ca [ref. [22])] are available. They are all of surface absorption form. The parameter values used in the analyses are summarized in table 2.

For the ^{6}Li particle, the potential parameters are not known very well. Especially for elastic scattering on p-shell nuclei, experiments have shown, that there exists a competing elastic multinucleon transfer as measured in ^{12}C(^{6}Li, ^{6}Li)^{12}C and ^{12}C (^{7}Li, ^{7}Li)^{12}C at 21 MeV lab [7]). We have adopted two kinds of parameter sets (type A and type B). The potential set A is obtained originally from the analysis of heavy-ion induced elastic scattering on ^{12}C, Voos *et al.* [26]). This potential is considered to be good also in describing the scattering of other strongly absorbed particles. It has a volume absorption form. The potential set B results from an analysis of 20 MeV

TABLE 2
Optical potential parameters used in the calculation

	Target		V	r_{0R}	a_R	W	r_{0I}	a_I	r_{0C}
d	^{10}B		118.0	0.863	0.916	5.44	1.59	0.716	1.3
	^{11}B		118.0	0.895	0.902	4.82	1.62	0.775	1.3
	^{12}C		117.1	0.9	0.982	14.0	1.8	0.405	1.3
	^{16}O		107.5	0.884	0.915	6.5	1.59	0.684	1.3
	^{19}F		92.2	0.965	0.888	8.9	1.46	0.813	1.3
	^{40}Ca		120.7	0.966	0.846	16.4	1.479	0.492	1.3
^{6}Li	parameter set	A	100.0	1.19	0.48	27.0	1.29	0.26	1.32
		B1	35.0	0.79	1.04	8.46	1.21	0.49	1.3
		B2	32.6	1.18	0.64	7.4	1.12	1.0	1.3

For deuteron optical potentials, the surface absorption form is used. For ^{6}Li two kinds of potential sets are used. Type A has a volume absorption form, type B a surface absorption form.

^{6}Li elastic scattering on ^{12}C (type B1) and ^{40}Ca (type B2) by Bethge *et al.* [27]). The surface absorption form is adopted in the present calculation because it seems to give better fits to elastic scattering data in ref. [27]).

5. Comparison with the experiment

In the previous sections, all parameters used in the DWBA calculation have been discussed and fixed, except for the parameters of the optical potentials describing the outgoing channel and the model to be used for the light residual nucleus ^{6}Li. We first

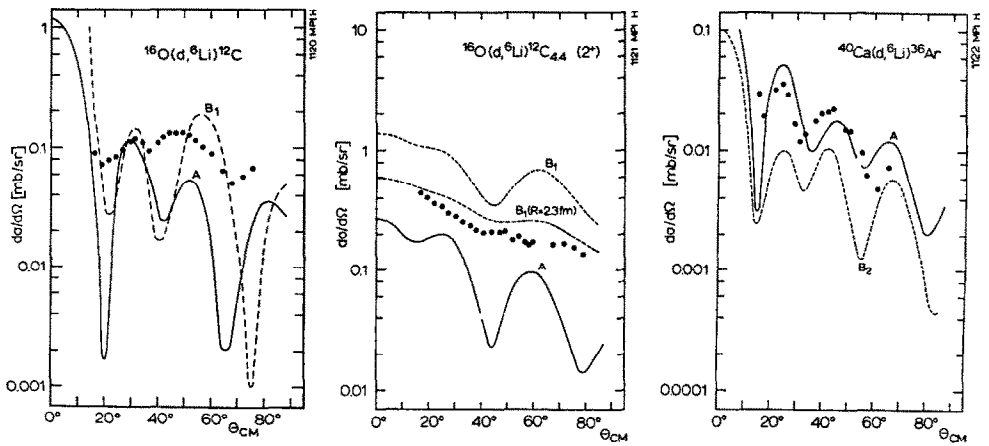

Fig. 7. Influence of the optical potential parameters for the exit channel on the calculated angular distributions. The potentials are given in table 2. For these calculations the cluster-model wave function Φ_{00} for ^{6}Li has been used and, where not otherwise indicated, the interaction radius is fixed at $R_D = 1.6$ fm.

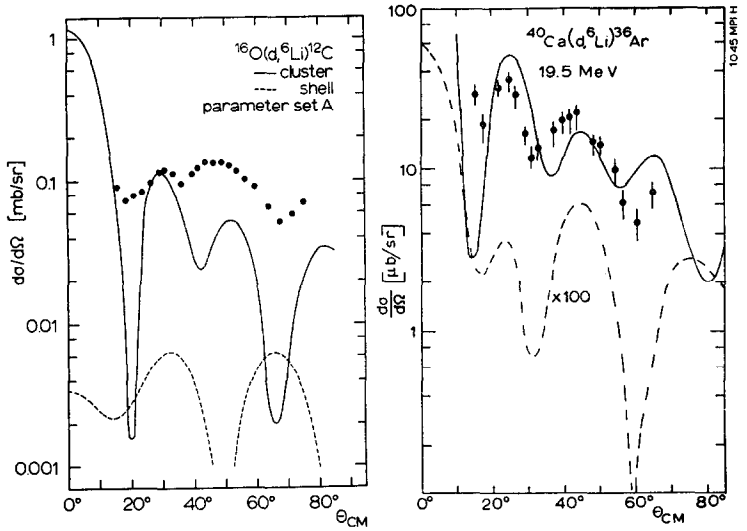

Fig. 8. Influence of the internal wave function of ^{6}Li on the calculated (d, ^{6}Li) cross section. For both calculations the optical potential parameter set A has been used.

discuss the influence of the different ^{6}Li potentials given in table 2 on the angular distributions of the (d, ^{6}Li) reaction. Fig. 7 shows some examples for the target nuclei ^{16}O and ^{40}Ca. Both ^{6}Li potentials lead to similar shapes of the angular distribution and to the same order of magnitude of the absolute cross section. For the following calculations, we have therefore confined ourselves to parameter set A, notwith-

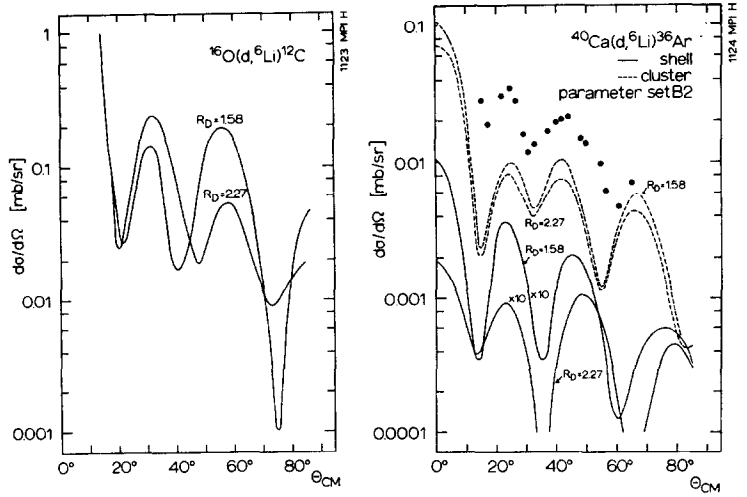

Fig. 9. Influence of interaction radius on the calculated angular distributions. For $^{16}O(d,^6Li)^{12}C$ the parameter set A and the wave function Φ_{00} was used.

standing the fact that we could get better fits in single cases by using different parameter sets, especially for the light target nuclei.

The influence of the internal wave function of ^{6}Li on the calculated (d, ^{6}Li) cross sections turns out to be much more important. As shown in fig. 8, both the

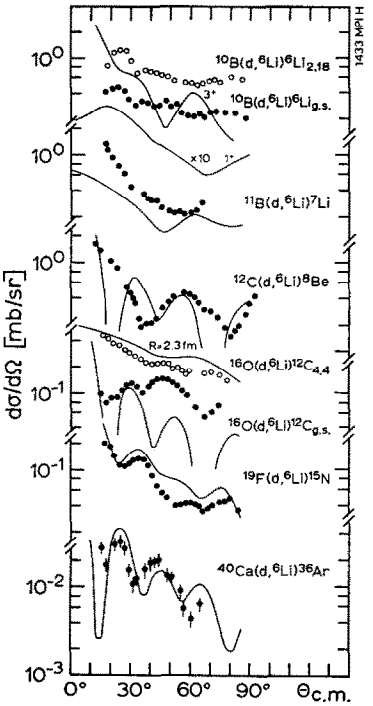

Fig. 10. Angular distributions for different (d, ^{6}Li) reactions and comparison with calculations using the cluster wave function Φ_{33} for ^{6}Li and the optical parameter set A.

shape of the angular distribution and the absolute cross section is changed drastically by using the shell-model wave function instead of the cluster model for ^{6}Li. The decrease of the theoretical cross section by about two orders of magnitude in the former case may be due to a destructive interference between the contributions of the surface and the inner part of the ^{6}Li form factor, which have different sign in the case of the shell model (see fig. 6).

The cluster-model assumption for ^{6}Li predicts the experimental cross sections correctly (fig. 8). The influence of the interaction radius R_D of eq. (12) determining the size of ^{6}Li was also checked (fig. 9). It was found that the theoretical cross sections vary only by about 30 % in the case of the reaction ^{40}Ca(d, ^{6}Li) when going from R_D = 1.56 fm to R_D = 2.27 fm. In the reaction ^{16}O(d, ^{6}Li)^{12}C the variation depends on the angle, but remains below a factor of 2 in forward direction. The value of R_D was therefore fixed at 1.6 fm.

The final calculations are shown in fig. 10. The comparison between theoretical and experimental cross sections is given in table 3. The theory predicts exactly the absolute cross sections of the (d, ^{6}Li) ground state transitions of the target nuclei from ^{11}B to ^{40}Ca. In particular, it reproduces the variation of the cross section by one order of magnitude between ^{11}B and ^{40}Ca.

TABLE 3

Comparison of theoretical and experimental cross sections

Reaction		l_{tr}	S_1	$\frac{d\sigma}{d\Omega}$ (μb/sr) calculated with Φ_{10}	Φ_{00}	1st maximum experiment
^{10}B(d, ^{6}Li)^{6}Li$_{G.S.}$	1^+	2	0.0035	6	30	500
		4	0.0113			
	3^+	0	0.208	239	700	1300
		2	0.205			
^{11}B(d, ^{6}Li)^{7}Li		0	0.206	200	400	600
		2	0.615			
^{12}C(d, ^{6}Li)^{8}Be		0	0.759	100	500	500
^{16}O(d, ^{6}Li)^{12}C$_{0+}$		0	0.333	6	140	140
^{19}F(d, ^{6}Li)^{15}N		1	0.088	8	170	140
^{40}Ca(d, ^{6}Li)^{36}Ar		0	0.0087	0.04	50	40

As seen from fig. 10 and table 3, the calculations are not able to describe the (d, ^{6}Li) reactions on the lightest nuclei; in particular, the absolute value of the measured cross section of the ^{10}B(d, ^{6}Li)^{6}Li ground state transition is much higher than predicted. This may be due to the following reasons:

(i) The lack of knowledge of the optical potential parameters of the ^{6}Li particle for lighter target nuclei. In fact the result of ref. [27]) shows that there exists a mass number dependence of the parameters.

(ii) The exchange effects that have been neglected in the present analyses. This effect may be more important, as one goes to lighter target nuclei.

(iii) A wrong description of ^{10}B by the shell model, i.e. a certain isolation of α and ^{6}Li in ^{10}B, as discussed in refs. [28,29]).

6. Summary

The (d, ^{6}Li) reaction on some p and sd shell nuclei has been measured and analyzed assuming a simple α-transfer. It was found that the experimental cross sections of the ground state transitions for all target nuclei except for ^{10}B can be reproduced quantitatively by the finite-range DWBA theory. This indicates that the assumption of shell-model wave functions used here for the target nuclei describes the spectroscopic

factors for α-clustering and transfer. The admixture of particle-hole components to the ground state of closed shell nuclei does not affect the cross section appreciably.

For the light residual nucleus ^{6}Li, in contrary, it was found that the shell model does not give an appropriate description. This was concluded from the fact that the resulting (d, ^{6}Li) cross sections are too small by two orders of magnitude compared to the experimental values. The validity of a cluster model for ^{6}Li is already suggested by the low energy for a separation into an α-particle and a deuteron. The analysis of electron scattering data showed the isolation of the α- and deuteron cluster in ^{6}Li. Therefore the influence of the cluster model on the form factor for (d, ^{6}Li) was investigated. For all (d, ^{6}Li) experiments, except ^{10}B, the calculations based on the cluster model reproduce very well the measured cross section. The discrepancy in the case of ^{10}B is assumed to be a hint for a certain isolation between the ^{6}Li and the α-cluster in ^{10}B, as suggested by cluster-model calculations [28]) and by the analysis of the (^{10}B, ^{6}Li) reaction [29]).

The authors are indebted to Prof. Gentner and Prof. Schmidt-Rohr for their interest and support. In particular one of us (H.Y.) is much indebted to them for making possible his stay at the institute and his studying there. Thanks are due to Mr. K. Hildenbrand and Mr. H. G. Bohlen for their help during the experiments. We wish to thank Dr. W. von Oertzen and Dr. F. Pühlhofer for useful discussions.

The DWBA calculations were performed using the IBM-360-44 computer of the University of Heidelberg.

References

1) W. von Oertzen, H. G. Bohlen, H. H. Gutbrod, K. D. Hildenbrand, U. C. Voos and R. Bock, Proc. Int. Conf. on nuclear reactions induced by heavy ions (North-Holland, Amsterdam, 1970) p. 156
2) V. G. Neudatchin, Proc. Int. Conf. on cluster phenomena in nuclei, Bochum (1969) B-2
3) L. J. Denes and W. W. Daehnick, Phys. Rev. **154** (1967) 928
4) J. B. Gerhard, P. Mizera and F. W. Slee, Annual Report Univ. of Washington (1964)
5) H. Yoshida, unpublished
6) I. Rotter, Nucl. Phys. **A122** (1968) 567; **A135** (1969) 378; Fortsch. der Phys. **16** (1968) 195
7) H. H. Gutbrod, K. Hildenbrand, W. von Oertzen, U. Voos and R. Bock, Proc. La Plagne Conf. (1969) II.5.1
8) K. Meier-Ewert, K. Bethge and K. O. Pfeiffer, Nucl. Phys. **A110** (1968) 142
9) G. Gaul, H. Lüdecke, R. Santo, H. Schmeing and R. Stock, Nucl. Phys. **A137** (1969) 177
10) J. B. French and B. J. Raz, Phys. Rev. **104** (1956) 1411
11) N. Austern, R. M. Drisko, E. C. Halbert and G. R. Satchler, Phys. Rev. **133** (1964) 33
12) P. J. A. Buttle and L. J. B. Goldfarb, Nucl. Phys. **78** (1966) 409;
T. Kammuri and H. Yoshida, Nucl. Phys. **A129** (1969) 625
13) M. A. K. Lodhi, Nucl. Phys. **A121** (1968) 549;
D. H. Lyons, Phys. Rev. **105** (1957) 936
14) V. V. Balashov and V. A. Eltekov, Nucl. Phys. **16** (1960) 423;
T. A. Brody, G. Jacob and M. Moshinsky, Nucl. Phys. **17** (1960) 16;
Yu. Smirnov, Nucl. Phys. **27** (1961) 177
15) C. L. Lin and S. Yoshida, Progr. Theor. Phys. **32** (1964) 885
16) J. M. Hansteen and H. W. Wittern, Phys. Lett. **24B** (1967) 381;
E. W. Schmid, Y. C. Tang and K. Wildermuth, Phys. Lett. **7** (1963) 263

17) A. N. Boyarkina, Bull. Acad. Sci. USSR (Sov. Phys.) **28** (1965) 255;
H. Ui, Phys. Rev. **161** (1967) 1099
18) D. Kurath, Phys. Rev. **101** (1956) 216;
T. Honda, H. Horie, Y. Kudo and H. Ui, Nucl. Phys. **62** (1965) 561
19) T. Inoue, T. Sebe, H. Hagiwara and A. Arima, Nucl. Phys. **59** (1964) 1
20) P. W. M. Glaudemans, G. Wiechers and P. J. Brussaard, Nucl. Phys. **56** (1964) 548
21) J. P. Elliot, J. Hope and H. A. Jahn, Phil. Trans. Roy. Soc. **246** (1953) 241
22) T. Honda, H. Horie, Y. Kudo and H. Ui, Prog. Theor. Phys. **31** (1964) 424; Phys. Lett. **10** (1964) 99
23) P. J. Ellis and L. Zamick, Ann. of Phys. **55** (1969) 61
24) W. Fitz, R. Jahr and R. Santo, Nucl. Phys. **A101** (1967) 449
25) R. H. Bassel, R. M. Drisko, G. R. Satchler, L. L. Lee, J. P. Schiffer and B. Zeidmann, Phys. Rev. **136** (1964) B960
26) U. C. Voos, W. von Oertzen and R. Bock, Nucl. Phys. **A135** (1969) 207
27) K. Bethge, C. M. Fou and R. W. Zurmühle, Nucl. Phys. **A123** (1969) 521
28) H. Hutzelmeyer and H. H. Hackenbroich, Proc. Int. Conf. on cluster phenomena in nuclei, Bochum (1969) PB5
29) K. D. Hildenbrand, H. H. Gutbrod, W. von Oertzen and R. Bock, Nucl. Phys. **A157** (1970) 297